Journal of Photochemistry and Photobiology A: Chemistry 214 (2010) 121–127

Contents lists available at ScienceDirect

Journal of Photochemistry and Photobiology A: Chemistry

journal homepage: www.elsevier.com/locate/jphotochem

# Theoretical study on photochemical behavior of *trans*-2-[4′-(dimethylamino)styryl]benzothiazole

Francis A.S. Chipem, Soumya Chatterjee, G. Krishnamoorthy*

*Department of Chemistry, Indian Institute of Technology Guwahati, Guwahati 781039, India*

ARTICLE INFO

*Article history:*
Received 4 February 2010
Accepted 16 June 2010
Available online 23 June 2010

*Keywords:*
TICT
TDDFT
Photophysics
Photoisomerization
Push–pull aromatic olefin

ABSTRACT

Photochemistry of *trans*-2-[4′-(dimethylamino)styryl]benzothiazole (*t*-DMASBT) has been examined theoretically. Ground state calculations are performed by density functional theory (DFT) method. For excited-state calculations restricted configuration interaction singles (RCIS) combined with time dependent DFT (TDDFT) approach was used. Theoretical calculations predicted the existence of two ground state conformers and the photophysics of both the conformers are nearly identical. With torsional rotation of dimethylamino group, the energies of $S_1$ and $S_2$ states increase, but that of $S_3$ state decreases. In contrary to an earlier report [J. Photochem. Photobiol. A: Chem. 195 (2008) 368–377], the calculation predicted at the perpendicular geometry the HOMO is localized on dimethylamino and, HOMO and LUMO are decoupled. Excitation from HOMO to LUMO at perpendicular geometry results in twisted intramolecular charge transfer (TICT) state. Avoided crossing of $S_3$ and $S_1$ states causes a barrier for formation of TICT state from locally excited state. Potential energy surface of isomerization constructed by TDDFT method suggests that the photoisomers are formed through phantom state in a nonradiative way, not by a radiative way from *cis* and *trans* isomers as proposed earlier by Saha et al. [J. Photochem. Photobiol. A: Chem. 199 (2008) 179–187].



## 1. Introduction

Excited-state torsional motion about carbon–carbon double bond that leads to *trans–cis* photoisomerization is an important nonradiative decay channel for many π-systems [1,2]. The photoisomerization has been known for several decades to dominate the photochemistry of aromatic olefins, and has been studied extensively and reviewed [1–5]. 'Push–pull' aromatic olefins are much more interesting [6–12]. The presence of single bonds linking electron donor and electron acceptor groups in 'push–pull' systems may allow twisted intramolecular charge transfer (TICT) state formation. On the other hand, the double bonds can also lead to *trans–cis* isomerization which can compete with TICT state formation.

*trans*-2-[4′-(Dimethylamino)styryl]benzothiazole (*t*-DMASBT) is a push–pull aromatic olefins, which has benzothiazole ring on one side of the olefin bond and dimethylanilino ring on the other side (Scheme 1). Fayed and Ali were the first to synthesize and study the photophysics of *t*-DMASBT [13]. They suggested that *t*-DMASBT is emitting from the intramolecular charge transfer (ICT) state and is due to increase in dipole moment in the $S_1$ state. Saha et al. had elaborated utility of *t*-DMASBT. It was found that the fluorophore can be used as molecular probe to study biological functions as well as biomimicking systems [14]. *t*-DMASBT can act as a surface probe to monitor the premicellar aggregation and the phase change during the process [15] and also it induces the formation of nanotubular suprastructures by cylclodextrins [16–18]. Saha et al. also reinvestigated DMASBT both experimentally and theoretically and proposed that DMASBT emits from TICT state in polar solvents [19]. They hypothesized that the $S_3$ state of the molecule developed a high dipole moment with twisting of dimethylamino group and thereby got stabilized in polar solvent to emit TICT fluorescence in polar solvents. But there is large overlap between the HOMO and LUMO (reported by Saha et al.) that involved in the formation of TICT state. However it is known [20,21] that under charge transfer conditions the donor and the acceptor are orbitally decoupled and therefore there is little or no overlap between the atomic orbitals contributing to the HOMO and those to the LUMO [12,22–24]. In addition the HOMO that is supposed to localize on the electron donating dimethylamino, is localized on the other parts of the molecules in the HOMO obtained by Saha et al. [19]. These behaviors of HOMO and LUMO in the formation of TICT state are unexpected. Saha et al. [14] also studied the photoisomerization of DMASBT and reported that the photoisomerization of DMASBT is different from that of stilbene and other olefins. According to their model the *cis–trans* isomerization occurs thermally in the first excited state and both the isomers relax to the ground state by radiative way. However

* Corresponding author. Tel.: +91 361 2582315; fax: +91 361 2582349.
*E-mail address:* gkrishna@iitg.ernet.in (G. Krishnamoorthy).

1010-6030/$ – see front matter © 2010 Elsevier B.V. All rights reserved.
doi:10.1016/j.jphotochem.2010.06.014

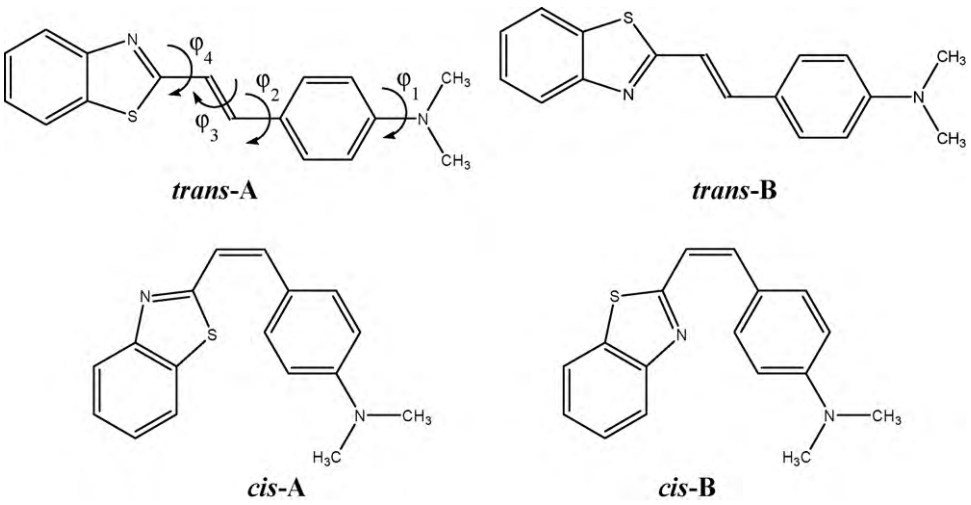


**Scheme 1.** Different molecular forms of DMASBT.

photoisomerization via phantom singlet state, $^1p^*$ was reported even in cases of many donor and acceptor substituted stilbenes [6–12].

Thus we reinvestigated theoretically the excited-state properties of DMASBT by time dependent density functional theory (TDDFT) to verify Saha et al. model about TICT emission and photoisomerization in DMASBT. Our theoretical calculations clearly suggest that HOMO is more localized on the donor dimethylamino group and the LUMO is localized on the rest of the molecule and there is a minimum overlap between these molecular orbitals. In addition the calculations predict that there is avoided crossing between the $S_3$ and $S_1$ states that makes a barrier for the formation of TICT state. In contrary to Saha et al. model the photoisomerization of DMASBT is also predicted to occur via perpendicular geometry in a nonradiative way.

## 2. Computational method

The molecular geometries in the ground state were obtained by full optimization of structural parameters employing Berny optimization algorithm by density functional calculation in spin restricted shell wavefunction manner [25,26]. The functional used in the calculation was B3LYP where the gradient corrected exchange functional of Becke [27] and the correlation functional of Lee, Yang and Paar (LYP) [28] were employed. The basis set used in all the calculations was 6-31G(d,p) which includes polarization functions, d orbitals for C, N, O and S atoms and p orbitals for H atoms.

Configuration interaction singles (CIS) [22,29] and complete active space self-consistent field (CASSCF) [30–32] methods are very popular computational methods for the excited-state electronic structures. CIS method is less expensive and found to overestimate the energies [33,34]. CASSCF method is also known to over estimate the excitation energy to ionic-type or charge transfer and it is necessary to include dynamic correlation to correct this behavior [32,35]. CASSCF are good for small systems, but quite expensive for large systems [30,31,36]. The geometries obtained at the CIS level as well as molecular properties are quite reasonable and correct, at least as a first approximation for a variety of molecules [34,37,38], including 4-dimethylaminobenzonitrile [39]. TDDFT calculations were also used successfully to explain the formation of the TICT state in systems like Michler's ketone and dimethylamino fluorenone [23,40]. In view of this we have performed ab initio CIS calculation to obtain the molecular geometry. As the energy predicted by the calculations are quite high compared to experimental values, using the CIS optimized geometries as input TDDFT calculations were employed to obtain the energies.

Vertical excitation energy calculations were performed on the optimized ground and excited $S_1$ state geometries for the assignment of excitation and emission energies, respectively, by TDDFT/B3LYP/6-31G(d,p) [41,42]. All the computations were performed with a developed version of Gaussian 03W [43].

## 3. Results and discussion

### 3.1. Conformers

Two conformers are possible for *t*-DMASBT (Scheme 1) and optimized geometrical parameters for both the conformers are compiled in Table 1. *Trans*-A is the most stable form of the molecule. However the energy difference between the two *trans* conformers is negligible, and DFT calculations predict a rotational barrier of 0.34 eV for the conversion of one conformer to other conformer (Fig. 1). Comparison of data in Table 1 shows that the geometrical parameters and properties of both the conformers are nearly same. The molecule is almost planar with small dihedral angle (~5°) between the dimethylamino group and rest of the molecule. The excitation energies were obtained by the vertical transition of the ground state geometries. The difference in excitation energies of both the conformer is very small and values obtained by TDDFT calculation are in excellent agreement with experimental value (Table 1). The longest wavelength transition is intense and has contribution only from HOMO–LUMO excitation and the transition is

**Table 1**
Optimized Parameters for *trans*-DMASBT in $S_0$ and $S_1$ states.

| Parameters | *trans*-A | | *trans*-B | |
|---|---|---|---|---|
| | $S_0$ | $S_1$ | $S_0$ | $S_1$ |
| Energy (eV)[a] | 0.0 | 3.2229 | 0.0009 | 3.2268 |
| T.E.[b] (nm) | 384 (384) | 419 (447) | 383 | 419 |
| Oscillator strength (*f*) | 1.3051 | 1.4833 | 1.3607 | 1.4881 |
| $\mu$ (D) | 5.2 | | 5.1 | |
| Dihedral angles (°) | | | | |
| $\varphi_1$ | 5.0 | 0.0 | 4.9 | 0.1 |
| $\varphi_2$ | 180.0 | 180.0 | 180.0 | 180.0 |
| $\varphi_3$ | 180.0 | 180.0 | 180.0 | 180.0 |
| $\varphi_4$ | 180.0 | 180.0 | 0.0 | 0.0 |

[a] With respect to ground state energy of *trans*-A.
[b] T.E.: transition energy and the values in parentheses are experimental value for *t*-DMAPBT in cyclohexane from Ref. [19].

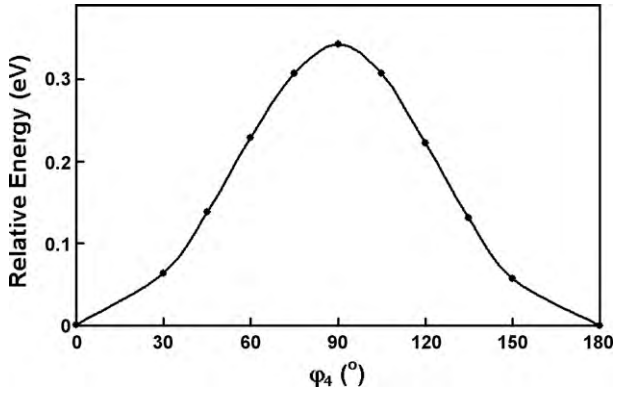


**Fig. 1.** Ground state potential energy surfaces for the conversion of *trans*-A to *trans*-B.

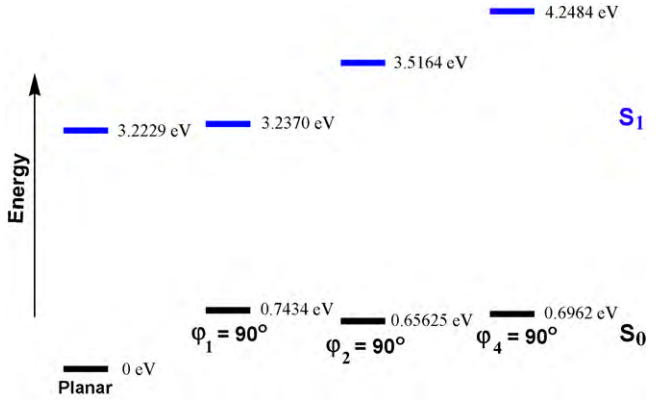


**Scheme 2.** Energy level diagram for planar and twisted conformers of *trans*-A. Similar results have been determined for *trans*-B (Supporting Information).

$\pi \rightarrow \pi^*$. The relaxed geometries in the excited state were obtained by full optimization using RCIS/6-31G(d,p). The excited-state optimized geometries indicate that the complete planarization of the molecule in the excited state and this is expected to increase the conjugation (Table 1). Thus, favors the quinioid structure in the excited state and responsible for the emission in nonpolar solvents. The emission energies are obtained by vertical transition from these relaxed geometries. The emission energies of both the conformers are same and also in good agreement with experimental value (Table 1).

### 3.2. TICT

DMASBT was reported to emit TICT emission only in polar solvents [19]. In the TICT state, donor is twisted from within the molecular plane to a position perpendicular to other part of the molecule [20,21]. In DMASBT the torsional rotation of the dimethylamino group ($\varphi_1$) or the dimethylanilino ring ($\varphi_2$) or the dimethylaminostyryl ring ($\varphi_3$) is supposed to result in TICT state. In a related system 4-dimethylamino,4′-cyanostilbene, it was proposed that the rotation of dimethylanilino leads to a TICT state and was stabilized by polar solvents [12]. However rotational motion of dimethylanilino group involves large amplitude motion and viscous solvents like glycerol retards the motion of such bulky moiety. It was found that the fluorescence yield of thioflavin T increases in glycerol, as it retards torsional motion of dimethylanilino group that is supposed to result in nonfluorescent TICT [44]. On the other hand TICT emission was observed for dimethylaminobenzonitrile even in polymer matrix, where the formation of TICT state involves the twisting motion of small dimethylamino group [45]. DMASBT emits strong TICT fluorescence in glycerol [14,19] and thus rule out rotation of bulky dimethylanilino group or dimethylaminostyryl moiety in the formation of TICT emission. However we have calculated the energy of all the three twisted conformers. The calculations also show that the formation of TICT state by the twisting of dimethylanilino group or dimethylaminostyryl group are energetically less favored compared to the twisting of dimethylamino group (Scheme 2). In *trans*-B conformer also rotations of bulky groups are unfavorable compared to that of dimethylamino group (Supporting Information).

The potential energy surface for the formation of TICT state was constructed by rotating the dimethylamino group from the relaxed excited state and performing partial optimization on different geometries that have preset torsional angles. The potential energy surfaces thus constructed are in Fig. 2 and the transition character of the first three excited states are compiled in Table 2. The frontier molecular orbitals involved in the transition for both planar and twisted states are shown in Fig. 3. From these it is clear that all the three states are $\pi\pi^*$ states. In the planar conformer as mentioned earlier, the $S_1$ state is described by HOMO–LUMO single excitation and is strongly allowed. But the higher states are composed of multiple excitations with small oscillator strength. The $S_2$ state has major contribution from HOMO-1–LUMO excitation with minor contribution from HOMO-2–LUMO and HOMO–LUMO+3. In the $S_3$ state HOMO-1–LUMO excitation has more contribution than the other excitations. But with rotation of dimethylamino group, the contribution of HOMO-1–LUMO excitation increases in the $S_3$ state and that of HOMO-2–LUMO excitation increases in the $S_2$ state. The energy of the $S_3$ state decreases and that of $S_2$ state increases with rotation of dimethylamino group. The two states cross each other at a torsional angle of ~50°. Alike $S_2$ state, the energy of $S_1$ state also increases with twisting. However the $S_3$ and $S_1$ states do not cross and there is an avoided crossing between these states. In the region of avoided crossing both states are expected to strongly mix up and finally repel each other, keeping their relative spectral positions unaltered. The $S_1$ state is defined by single excitation up to 50° rotation of dimethylamino group. When the twisting angle increases further, the $S_1$ state has additional contribution from HOMO-1–LUMO excitation. The same way HOMO–LUMO excitation also contributes to $S_3$ state when torsional rotation increases above 50°. The oscillator strength of $S_1$ state decreases and that of $S_3$ state increases. Finally when the states move apart at 90°, the $S_1$ and $S_3$ states have contribution only from single excitations. Saha et al. [19] also suggested that the energy of the $S_3$ state decreases with torsional motion of dimethylamino group, but they reported that the $S_3$ and $S_1$ states also cross each other, in contrary to avoided crossing between these

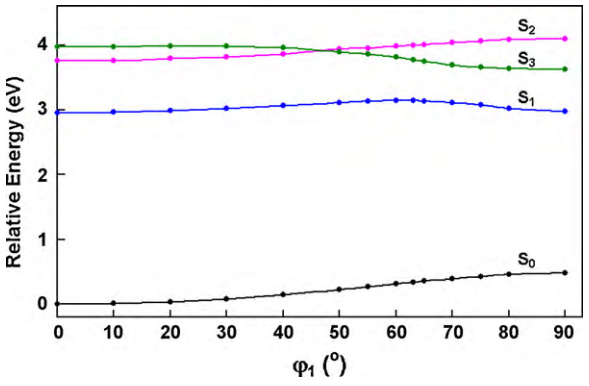


**Fig. 2.** Simulated potential energy surfaces for the formation of TICT state obtained by the torsional motion of dimethylamino group in *trans*-A. Similar results have been determined for *trans*-B (Supporting Information).

**Table 2**
Transition character of different energy level on the pathway to the TICT state in *trans*-A.

| Dihedral angle, $\varphi_1$ (°) | $S_1$ state | | $S_2$ state | | $S_3$ state | |
|---|---|---|---|---|---|---|
| | MO | T.E. (*f*)[a] | MO | T.E. (*f*)[a] | MO | T.E. (*f*)[a] |
| 0 | LUMO ← HOMO (100%) | 2.960 (1.48) | LUMO ← HOMO-2 (35.7%)<br>LUMO ← HOMO-1 (52.2%)<br>LUMO+2 ← HOMO (12.1%) | 3.757 (0.04) | LUMO ← HOMO-2 (38.4%)<br>LUMO ← HOMO-1 (25.1%)<br>LUMO+1 ← HOMO (11.1%)<br>LUMO+2 ← HOMO (9.8%)<br>LUMO+3 ← HOMO (15.6%) | 3.973 (0.00) |
| 10 | LUMO ← HOMO (100%) | 2.957 (1.48) | LUMO ← HOMO-2 (37.7%)<br>LUMO ← HOMO-1 (50.5%)<br>LUMO+2 ← HOMO (11.8%) | 3.756 (0.04) | LUMO ← HOMO-2 (37.3%)<br>LUMO ← HOMO-1 (26.6%)<br>LUMO+1 ← HOMO (10.9%)<br>LUMO+2 ← HOMO (10.0%)<br>LUMO+3 ← HOMO (15.2%) | 3.966 (0.01) |
| 20 | LUMO ← HOMO (100%) | 2.950 (1.48) | LUMO ← HOMO-2 (44.2%)<br>LUMO ← HOMO-1 (44.7%)<br>LUMO+2 → HOMO (11.1%) | 3.750 (0.04) | LUMO ← HOMO-2 (33.2%)<br>LUMO ← HOMO-1 (43.1%)<br>LUMO+1 ← HOMO (10.3%)<br>LUMO+2 ← HOMO (10.7%)<br>LUMO+3 ← HOMO (14.2%) | 3.942 (0.01) |
| 30 | LUMO ← HOMO (100%) | 2.937(1.46) | LUMO ← HOMO-2 (62.9%)<br>LUMO ← HOMO-1 (37.1%) | 3.737 (0.04) | LUMO ← HOMO-2 (25.1%)<br>LUMO ← HOMO-1 (40.8%)<br>LUMO+1 ← HOMO (9.5%)<br>LUMO+2 ← HOMO (12.8%)<br>LUMO+3 ← HOMO (11.8%) | 3.897 (0.02) |
| 40 | LUMO ← HOMO (100%) | 2.916 (1.42) | LUMO ← HOMO-2 (72.6%)<br>LUMO ← HOMO-1 (14.6%)<br>LUMO+3 → HOMO (12.8%) | 3.714 (0.03) | LUMO ← HOMO-2 (12.9%)<br>LUMO ← HOMO-1 (60.1%)<br>LUMO+1 ← HOMO (9.9%)<br>LUMO+2 ← HOMO (17.2%) | 3.819 (0.05) |
| 50 | LUMO ← HOMO (100%) | 2.883 (1.32) | LUMO ← HOMO-2 (37.4%)<br>LUMO ← HOMO-1 (49.8%)<br>LUMO+2 ← HOMO (12.8%) | 3.708 (0.13) | LUMO ← HOMO-2 (52.7%)<br>LUMO ← HOMO-1 (36.7%)<br>LUMO+3 → HOMO (10.6%) | 3.669 (0.02) |
| 60 | LUMO ← HOMO-1 (21.5%)<br>LUMO ← HOMO (78.5%) | 2.825 (1.07) | LUMO ← HOMO-2 (72.0%)<br>LUMO ← HOMO-1 (16.6%)<br>LUMO+3 ← HOMO (11.3%) | 3.666 (0.07) | LUMO ← HOMO-2 (19.2%)<br>LUMO ← HOMO-1 (69.6%)<br>LUMO ← HOMO (11.2%) | 3.497 (0.28) |
| 70 | LUMO ← HOMO-1 (33.4%)<br>LUMO ← HOMO (66.6%) | 2.718 (0.60) | LUMO ← HOMO-2 (100%) | 3.642 (0.06) | LUMO ← HOMO-2 (12%)<br>LUMO ← HOMO-1 (64.6%)<br>LUMO ← HOMO (23.4%) | 3.299 (0.73) |
| 80 | LUMO ← HOMO-1 (40.9%)<br>LUMO ← HOMO (59.1%) | 2.568 (0.15) | LUMO ← HOMO-2 (100%) | 3.626 (0.06) | LUMO ← HOMO-1 (62.9%)<br>LUMO ← HOMO (37.1%) | 3.179 (1.16) |
| 90 | LUMO ← HOMO (100%) | 2.494 (0.00) | LUMO ← HOMO-2 (84.7%)<br>LUMO+3 ← HOMO-1 (15.3%) | 3.620 (0.06) | LUMO ← HOMO-1 (100%) | 3.144 (1.30) |

[a] T.E.: transition energy in eV, *f*: oscillator strength.

two states predicted by the present study. They considered only *trans*-B conformer in their calculation. However the present calculations predicted that the behavior for the first three excited states of *trans*-B conformer is also nearly identical to that of *trans*-A conformer (Supporting Information). In both *trans*-A and *trans*-B, at 90°, the lowest singlet excited state is defined by HOMO–LUMO single excitation. The HOMO is localized on the charge donating dimethylamino group and the LUMO is localized on the acceptor (Fig. 3). Thus it is clear that the orbitals are decoupled at perpendicular geometry and the HOMO–LUMO excitation ensures a full electron transfer that results in the formation of TICT state. The avoided crossing causes a barrier for the formation of TICT state from the locally excited state in *t*-DMASBT. The barrier height and the energy of the TICT state are expected to decrease with increase in polarity to favor the formation of TICT state in polar solvents.

Recently it has been suggested that for DMABN the TICT state is directly formed from the Frank-Condon structure on $S_2$ through a conical intersection, corresponding to a nearly barrierless TICT-forming pathway in a nonadiabatic way [46,47]. However the present calculations predicted that the formation of TICT state in *t*-DMASBT is an adiabatic process. It was suggested for *trans*-aminostilbenes [11], the systems similar to *t*-DMASBT that the nonadiabatic process has no role in the formation of TICT state. This was due to the different electronic structures in aminostilbenes from the DMABN systems and the argument also holds good for *t*-DMASBT.

### 3.3. Photoisomerization

Torsional rotational around C=C bond that leads to *cis–trans* isomerization is one of the important de-excitation path in aryl olefins and is competing with radiative decays [1–5]. In general, the torsional rotation in either the singlet or the triplet excited-state reaches a potential minimum phantom state ($^1p^*$ or $^3p^*$), at the perpendicular geometry. The decay of $^1p^*$ and $^3p^*$ partitions to *trans* and *cis* isomers with nearly equal probability. Saha et al. studied the effect of viscosity and temperature on the fluorescence quantum yield of *t*-DMASBT [14]. Their studies revealed that the fluorescence yield increases with increase in viscosity and decreases with increase in temperature. They had performed AM1 calculations to predict the potential energy surface for isomerization. The potential energy surface constructed by them have barrier of 77 kcal mol$^{-1}$ in the ground state and the barrier height was at the torsional angle of ~40°. The shape of the potential barrier in the $S_1$ state is nearly identical to that of $S_0$ state, but the height of the barrier was reduced to 36 kcal mol$^{-1}$ at ~40°. In contrary to those

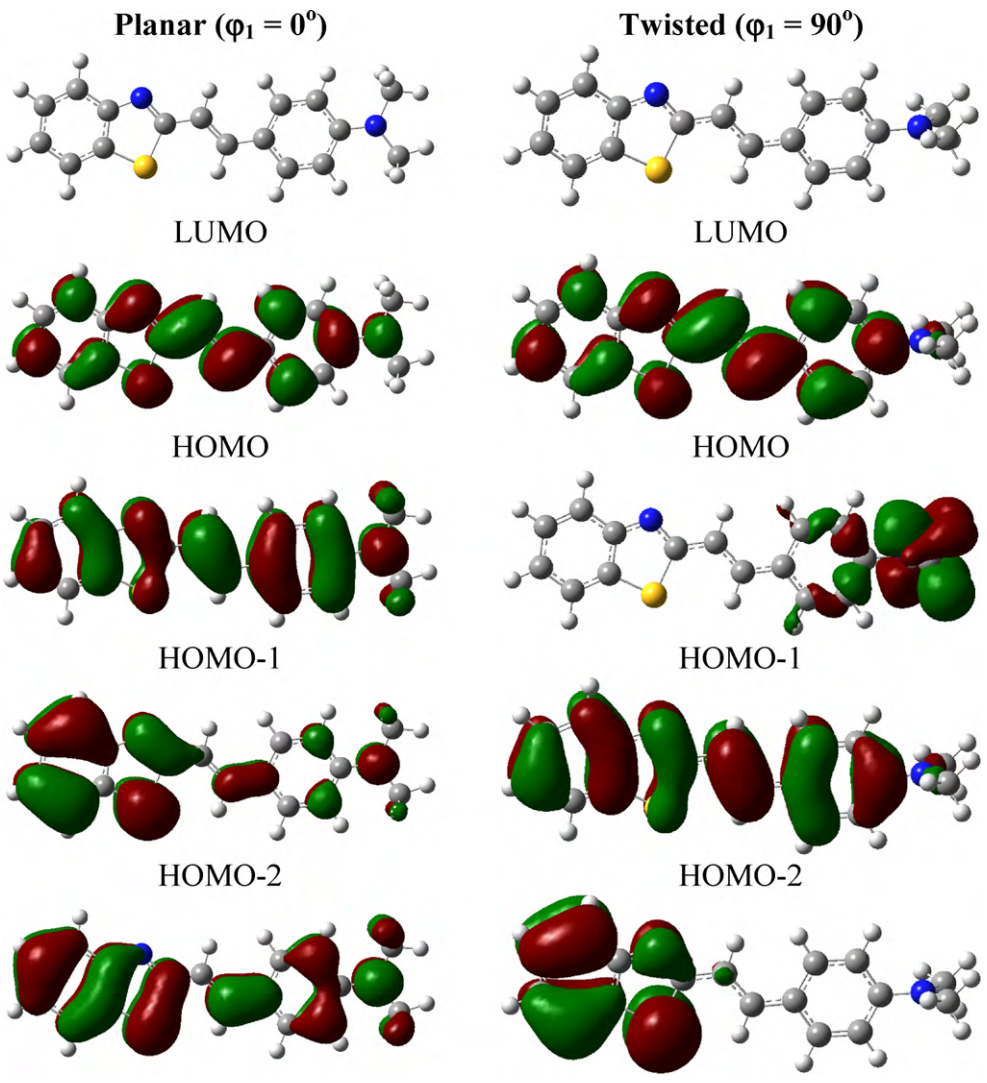


**Fig. 3.** Optimized structure and the isosurface plot of frontier molecular orbitals obtained by TDDFT calculation for planar ($\varphi_1 = 0^\circ$) and twisted ($\varphi_1 = 90^\circ$) conformers of *trans*-A. Similar results have been determined for *trans*-B (Supporting Information).

observed for aryl olefin no perpendicular minimum was observed in the potential energy surface obtained by Saha et al. It was proposed that DMASBT undergo temperature induced photoisomerization and fluorescence emission from both the isomer.

We have constructed the potential energy surface for isomerization from the Franck–Condon state of both the *trans* conformers using TDDFT method by rotating the olefinic bond in the excited state. The potential energy surfaces thus obtained are shown in Fig. 4 and are quite different from those reported by Saha et al. [14]. The perpendicular geometry possesses the maximum energy in ground state, but has the minimum energy in the $S_1$ state. There is a small barrier for *trans* isomer and little or no barrier for *cis* isomer to reach the perpendicular minimum, the phantom state, from there the molecule is expected to decay nonradiatively with nearly equal probability to *trans* and *cis* isomers. The picture is consistent with those observed for stilbene and other aromatic

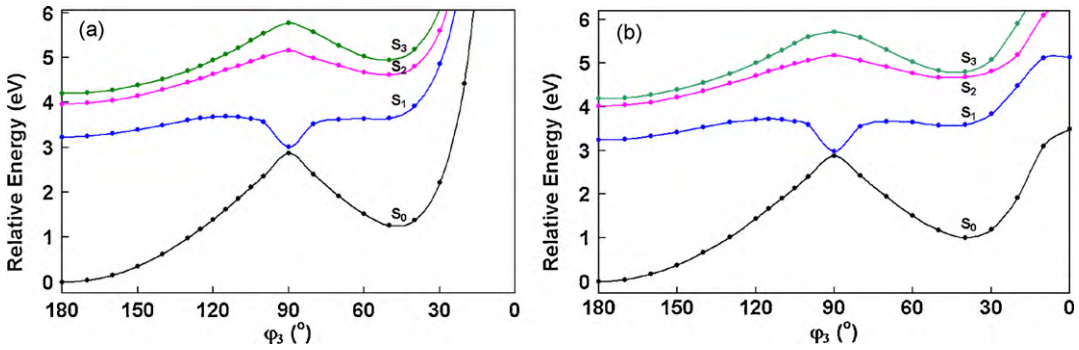


**Fig. 4.** Potential energy surfaces simulated for photoisomerization of (a) *trans*-A and (b) *trans*-B.

olefins [1,2]. The formation of the phantom state is energetically more favored than the formation of TICT state. This explains the low fluorescence quantum yield of *t*-DMASBT in nonpolar solvents [14].

## 4. Conclusion

The *t*-DMASBT exists in two conformeric forms. The difference in energy and dipole moment are very little between the conformers. The excitation and emission energies calculated by TDDFT method is in good agreement with the experimental values. Twisting of dimethylanilino and dimethylanilinostyryl moieties are high energy process compared to twisting of dimethylamino group. The $S_3$ state gets stabilized with torsional rotation of dimethylamino and it crosses the $S_2$ state, but there is an avoided crossing between $S_3$ and $S_1$ states. At perpendicular geometry, the HOMO is localized on the dimethylamino group and thus, the donor lone pair becomes available for charge transfer to decoupled LUMO that results in the TICT state. *t*-DMASBT undergoes photoisomerization in the $S_1$ state through phantom state, and is a major nonradiative path of de-excitation. In nonpolar solvents *cis–trans* isomerization is the dominating process and in polar solvents it is expected to compete with TICT process.

## Acknowledgements

The work is supported through project funding by Council for Scientific and Industrial Research (CSIR), India ((01(2082)/06/EMR-II) and Department of Science and Technology, India (SR/S1/PC-19/2006). Francis acknowledges CSIR, India for the research fellowship.

## Appendix A. Supplementary data

Supplementary data associated with this article can be found, in the online version, at doi:10.1016/j.jphotochem.2010.06.014.

## References

[1] J. Saltiel, J.L. Charlton, Cis–trans isomerization of olefins, in: P. de Mayo (Ed.), Rearrangements in Ground and Excited States, Vol. 3, Academic Press, New York, 1980, pp. 25–89.
[2] D.H. Waldeck, Photoisomerization dynamics of stilbenes, Chem. Rev. 91 (1991) 415–436.
[3] M. Zimmer, Non-retinal chromophoric proteins, in: C. Dugave (Ed.), Cis–Trans Isomerization in Biochemistry, Wiley–VCH, Weinheim, 2006, pp. 77–94.
[4] J.-S. Yang, G.-J. Huang, Y.-H. Liu, S.-M. Peng, Photoisomerization of the green fluorescence protein chromophore and the meta- and para-amino analogues, Chem. Commun. (2008) 1344–1346.
[5] C. Dugave, L. Demange, Cis–trans isomerization of organic molecules and biomolecules: implications and applications, Chem. Rev. 103 (2003) 2475–2532.
[6] H. Le Breton, B. Bennetau, J.-F. Letard, R. Lapouyade, W. Rettig, Nonradiative twisted intramolecular charge transfer state in polar stilbenes: photophysical study of 4-perfluorooctylsulfonyl-4′-N,N-dimethylamino stilbene and two bridged derivatives, J. Photochem. Photobiol. A: Chem. 95 (1996) 7–20.
[7] M. Dekhtyar, W. Rettig, Charge-transfer transitions in twisted stilbenoids: interchangeable features and generic distinctions of single- and double-bond twists, J. Phys. Chem. A 111 (2007) 2035–2039.
[8] A. Sczepan, W. Rettig, A.I. Tolmachev, V.V. Kurdyukov, The role of internal twisting in the photophysics of stilbazolium dyes, Phys. Chem. Chem. Phys. 3 (2001) 3555–3561.
[9] H. Braatz, S. Hecht, H. Seifert, S. Helm, J. Bendig, W. Rettig, Photochemistry and photophysics of donor-acceptor-polyenes. I: all-trans-4-dimethylamino-4′-cyano-1,4-diphenylbutadiene (DCB), J. Photochem. Photobiol. A: Chem. 123 (1999) 99–108.
[10] X.-M. Wang, Y.-F. Zhou, W.-T. Yu, C. Wang, Q. Fang, M.-H. Jiang, H. Leib, H.-Z. Wang, Two-photon pumped lasing stilbene-type chromophores containing various terminal donor groups: relationship between lasing efficiency and intramolecular charge transfer, J. Mater. Chem. 10 (2000) 2698–2703.
[11] J.-S. Yang, K.-L. Liau, C.-M. Wang, C.-Y. Hwang, Substituent-dependent photoinduced intramolecular charge transfer in N-aryl-substituted trans-4-aminostilbenes, J. Am. Chem. Soc. 126 (2004) 12325–12335.
[12] Y. Amatatsu, Ab initio study on the photochemical behavior of 4-dimethylamino, 4′-cyanostilbene, Chem. Phys. 274 (2001) 87–98.
[13] T.A. Fayed, S.S. Ali, Protonation dependent photoinduced intramolecular charge transfer in 2-(p-dimethylaminostyryl)benzazoles, Spectrosc. Lett. 36 (2003) 375–386.
[14] S.K. Saha, P. Purkayastha, A.B. Das, Excited state isomerization and effect of viscosity- and temperature-dependent torsional relaxation on TICT fluorescence of trans-2-[4-(dimethylamino)styryl]benzothiazole, J. Photochem. Photobiol. A: Chem. 199 (2008) 179–187.
[15] S.S. Jaffer, M. Sowmiya, S.K. Saha, P. Purkayastha, Defining the different phases of premicellar aggregation using the photophysical changes of a surface-probing compound, J. Colloids Interface Sci. 325 (2008) 236–242.
[16] S.S. Jaffer, S.K. Saha, G. Eranna, A.K. Sharma, P. Purkayastha, Intramolecular charge transfer probe induced formation of α-cyclodextrin nanotubular suprastructures: a concentration dependent process, J. Phys. Chem. C 112 (2008) 11199–11204.
[17] M. Sowmiya, P. Purkayastha, S.K. Saha, S.S. Jaffer, Characterization of guest molecule concentration dependent nanotubes of β-cyclodextrin and their secondary assembly: study with trans-2-[4-(dimethylamino)styryl] benzothiazole, a TICT-fluorescence probe, J. Photochem. Photobiol. A: Chem. 205 (2009) 186–196.
[18] S.S. Jaffer, S.K. Saha, P. Purkayastha, Fragmentation of molecule-induced γ-cyclodextrin nanotubular suprastructures due to drug dosage, J. Colloids Interface Sci. 337 (2009) 294–299.
[19] S.K. Saha, P. Purkayastha, A.B. Das, Photophysical characterization and effect of pH on the twisted intramolecular charge transfer fluorescence of trans-2-[4-(dimethylamino)styryl]benzothiazole, J. Photochem. Photobiol. A: Chem. 195 (2008) 368–377.
[20] W. Rettig, Charge separation in excited states of decoupled systems—TICT compounds and implications regarding the development of new laser dyes and the primary process of vision and photosynthesis, Angew. Chem. Int. Ed. Engl. 25 (1986) 971–988.
[21] Z.R. Grabowski, K. Rotkiewicz, W. Rettig, Structural changes accompanying intramolecular electron transfer: focus on twisted intramolecular charge-transfer states and structures, Chem. Rev. 103 (2003) 3899–4302.
[22] D. LeGourriérec, V. Kharlanov, R.G. Brown, W. Rettig, Excited-state intramolecular proton transfer (ESIPT) in 2-(2′-hydroxyphenyl)-oxazole and -thiazole, J. Photochem. Photobiol. A: Chem. 130 (2000) 101–111.
[23] T. Pal, M. Paul, S. Ghosh, Study of intramolecular charge transfer of Michler's ketone using time dependent density functional theory, J. Mol. Struct. (THEOCHEM) 860 (2008) 8–12.
[24] F.A.S. Chipem, G. Krishnamoorthy, Comparative theoretical study of rotamerism and excited state intramolecular proton transfer of 2-(2′-hydroxyphenyl)benzimidazole, 2-(2′-hydroxyphenyl)imidazo[4,5-b]pyridine, 2-(2′-hydroxyphenyl)imidazo[4,5-c]pyridine and 8-(2′-hydroxyphenyl)purine, J. Phys. Chem. A 113 (2009) 12063–12070.
[25] P. Hohenberg, W. Kohn, Inhomogeneous electron gas, Phys. Rev. B 136 (1964) 864–871.
[26] W. Kohn, L. Sham, Self-consistent equations including exchange and correlation effects, J. Phys. Rev. A 140 (1965) 1133–1138.
[27] A.D. Becke, Density-functional thermochemistry. 3. The role of exact exchange, J. Chem. Phys. 98 (1993) 5648–5652.
[28] C. Lee, W. Yang, R.G. Parr, Development of the Colle-Savetti correlation-energy formula into a functional of the electron-density, Phys. Rev. B 37 (1988) 785–789.
[29] Y. Wu, P.V. Lawson, M.M. Henary, K. Schmidt, J.-L. Brédas, C.J. Fahrni, Excited state intramolecular proton transfer in 2-(2′-arylsulfonamidophenyl)benzimidazole derivatives: insights into the origin of donor substituent-induced emission energy shifts, J. Phys. Chem. A 111 (2007) 4584–4595.
[30] P.-A. Malmqvist, B.O. Roos, The CASSCF state interaction method, Chem. Phys. Lett. 155 (1989) 189–194.
[31] J. Stalring, A. Bernhardsson, R. Lindh, Analytical gradients of a state average MCSCF state and a state average diagnostic, Mol. Phys. 99 (2001) 103–114.
[32] M.J. Paterson, M.A. Robb, L. Blancafort, A.D. DeBellis, Theoretical study of benzotriazole UV photostability: ultrafast deactivation through coupled proton and electron transfer triggered by a charge-transfer state, J. Am. Chem. Soc. 126 (2004) 2912–2922.
[33] V.I. Stsiapura, A.A. Maskevich, V.A. Kuzmitsky, K.K. Turoverov, I.M. Kuznetsova, Computational study of thioflavin T torsional relaxation in the excited state, J. Phys. Chem. A 111 (2007) 4829–4835.
[34] J.F. Stanton, J. Gauss, N. Ishikawa, M. Head-Gordon, A comparison of single reference methods for characterizing stationary points of excited state potential energy surfaces, J. Chem. Phys. 103 (1995) 4160–4174.
[35] L. Serrano-Andres, B. Roos, Theoretical study of the absorption and emission spectra of indole in the gas phase and in a solvent, J. Am. Chem. Soc. 118 (1996) 185–195.
[36] M.J. Paterson, M.A. Robb, L. Blancafort, A.D. DeBellis, Mechanism of an exceptional class of photostabilizers: a seam of conical intersection parallel to excited state intramolecular proton transfer (ESIPT) in o-hydroxyphenyl-(1,3,5)-triazine, J. Phys. Chem. A 109 (2005) 7527–7537.
[37] C.M. Gittins, E.A. Rohlfing, C.M. Rohlfing, Experimental and theoretical characterization of the $S_1$–$S_0$ transition of benzo[a]pyrene, J. Chem. Phys. 105 (1996) 7323–7335.
[38] K.B. Wiberg, Y. Wang, A.E. de Oliveira, S.A. Perera, P.H. Vaccaro, Comparison of CIS- and EOM-CCSD-calculated adiabatic excited-state structures. Changes in

charge density on going to adiabatic excited states, J. Phys. Chem. A 109 (2005) 466–477.
[39] A.B.J. Parusel, W. Rettig, W. Sudholt, A comparative theoretical study on DMABN: significance of excited state optimized geometries and direct comparison of methodologies, J. Phys. Chem. A 106 (2002) 804–815.
[40] G.J. Zhao, K.L. Han, Role of intramolecular and intermolecular hydrogen bonding in both singlet and triplet excited states of aminofluorenones on internal conversion, intersystem crossing, and twisted intramolecular charge transfer, J. Phys. Chem. A 113 (2009) 14329–14335.
[41] M.E. Casida, Time-dependent density functional response theory for molecules, in: D.P. Chong (Ed.), Recent Advances in Density Functional Methods Part I, World Scientific, Singapore, 1995, pp. 155–192.
[42] E.K.U. Gross, J.F. Dobson, M. Petersilka, Density functional theory of time-dependent phenomena, Top. Curr. Chem. 118 (1996) 81–172.
[43] M.J. Frisch, G.W. Trucks, H.B. Schlegel, G.E. Scuseria, M.A. Robb, J.R. Cheeseman, J.A. Montgomery Jr., T. Vreven, K.N. Kudin, J.C. Burant, J.M. Millam, S.S. Iyengar, J. Tomasi, V. Barone, B. Mennucci, M. Cossi, G. Scalmani, N. Rega, G.A. Petersson, H. Nakatsuji, M. Hada, M. Ehara, K. Toyota, R. Fukuda, J. Hasegawa, M. Ishida, T. Nakajima, Y. Honda, O. Kitao, H. Nakai, M. Klene, X. Li, J.E. Knox, H.P. Hratchian, J.B. Cross, V. Bakken, C. Adamo, J. Jaramillo, R. Gomperts, R.E. Stratmann, O. Yazyev, A.J. Austin, R. Cammi, C. Pomelli, J.W. Ochterski, P.Y. Ayala, K. Morokuma, G.A. Voth, P. Salvador, J.J. Dannenberg, V.G. Zakrzewski, S. Dapprich, A.D. Daniels, M.C. Strain, O. Farkas, D.K. Malick, A.D. Rabuck, K. Raghavachari, J.B. Foresman, J.V. Ortiz, Q. Cui, A.G. Baboul, S. Clifford, J. Cioslowski, B.B. Stefanov, G. Liu, A. Liashenko, P. Piskorz, I. Komaromi, R.L. Martin, D.J. Fox, T. Keith, M.A. Al-Laham, C.Y. Peng, A. Nanayakkara, M. Challacombe, P.M.W. Gill, B. Johnson, W. Chen, M.W. Wong, C. Gonzalez, J.A. Pople, Gaussian 03, Revision E.01, Gaussian, Inc., Wallingford, CT, 2004.
[44] V.I. Stsiapura, A.A. Maskevich, V.A. Kuzmitsky, V.N. Uversky, I.M. Kuznetsova, K.K. Turoverov, Thioflavin T as a molecular rotor: fluorescent properties of thioflavin T in solvents with different viscosity, J. Phys. Chem. B 112 (2008) 15893–15902.
[45] C. Cazeau-Dubroca, A. Peirigua, S. Ait-Lyazidi, G. Nouchi, P. Cazeau, R. Lapouyade, TICT fluorescence in rigid matrices: α-delayed fluorescence, Chem. Phys. Lett. 124 (1986) 110–115.
[46] W. Fuß, K.K. Pushpa, W. Rettig, W.E. Schmid, S.A. Trushin, Ultrafast charge transfer via a conical intersection in dimethylaminobenzonitrile, Photochem. Photobiol. Sci. 1 (2002) 255–262.
[47] I. Gomez, M. Reguero, M. Boggio-Pasqua, M.A. Robb, Intramolecular charge transfer in 4-aminobenzonitriles does not necessarily need the twist, J. Am. Chem. Soc. 127 (2005) 7119–7129.